

Application of the group contribution volume translated Peng-Robinson equation of state to new commercial refrigerant mixtures[☆]

I. H. Bell^{a,*}, J. Welliquet^b, M. E. Mondejar^c, A. Bazyleva^a, S. Quoilin^d, F. Haglind^c

^aApplied Chemicals and Materials Division, National Institute of Standards and Technology, Boulder, CO 80305, USA

^bEnergy Systems Research Unit, University of Liège, Liège, Belgium

^cDepartment of Mechanical Engineering, Technical University of Denmark, Building 403, 2800 Kongens Lyngby, Denmark

^dDepartment of Mechanical Engineering, KU Leuven, Geel. Kleinhoefstraat 4. 2440 Geel, Belgium

Abstract

This work evaluates the performance of the group contribution volume translated Peng-Robinson model when predicting the vapor-liquid equilibrium and single phase densities of 28 commercial refrigerant mixtures with low global warming potential and zero ozone depletion potential. Cubic equations of state, and particularly the Peng-Robinson equation of state, are widely used in the refrigeration industry due to their easy applicability for new substances, and their low computational time, although generally lower prediction accuracies must be expected compared to multiparameter equations of state. The group contribution volume translated Peng-Robinson equation of state combines the Peng-Robinson equation of state with a new attraction term, improved mixing rules using a group contribution approach, and volume translation. The results are compared with the estimates obtained using the non translated Peng-Robinson equation of state, and a multiparameter equation of state.

Keywords: Cubic equation of state, Peng-Robinson, GC-VTPR, UNIFAC, refrigerant mixtures.

1. Introduction

The current search for sustainable and environmentally friendly refrigerants is driven by the recent approval of increasingly restrictive regulations that limit the use of substances with high global warming potential (GWP), and the need to maintain high process efficiencies. In this context, mixtures containing new refrigerants with low GWP are of special importance, since their use offers new degrees of freedom that

allow for the optimization of their composition to tune their properties. However, experimental data of the thermophysical properties of new refrigerants are scarce, and it is even scarcer for their mixtures. The lack of experimental data makes it unfeasible to develop complex multiparameter equations of state (EoSs) (such as those available in the state of the art thermophysical property library REFPROP (Lemmon et al., 2018)) and to ensure high accuracy of the predictions. This fact introduces additional uncertainty in the prediction of the performance of new refrigerants, and the evaluation of their prospects as future replacement refrigerants. In this context it is essential to develop mixture models that, requiring little to no experimental data of the novel refrigerants, are able to estimate their thermophysical behavior with sufficient accuracy.

[☆]Contribution of the National Institute of Standards and Technology, not subject to copyright in the US

*Corresponding author

Email addresses: ian.bell@nist.gov (I. H. Bell), j.welliquet@alumni.ulg.ac.be (J. Welliquet), maemmo@mek.dtu.dk (M. E. Mondejar), ala.bazyleva@nist.gov (A. Bazyleva), sylvain.quoilin@kuleuven.be (S. Quoilin), frh@mek.dtu.dk (F. Haglind)



1 Cubic equations of state (cEoS) have been widely 40
2 used in the simulation of chemical industrial pro- 41
3 cesses and in the oil extraction industry because they 42
4 require only a very general knowledge of the fluid 43
5 molecule and allow for fast computational times. Al- 44
6 though it is well known that cEoS fail in the predic- 45
7 tion of liquid densities, and near the critical point, 46
8 as well as in the prediction of properties of polar 47
9 substances, a number of new cEoS have been devel- 48
10 oped in order to improve their accuracy for specific 49
11 cases. However, when used for the estimation of 50
12 mixture properties, cEoS require the use of mixing 51
13 rules that contain parameters which are commonly 52
14 fitted from experimental data for specific fluids. This 53
15 can represent a problem when one or more of the 54
16 mixture components is a relatively newly introduced 55
17 substance for which there are minimal experimental 56
18 measurements. 57

19 In principle, there are two types of mixing rules 58
20 for cEoS, which are the van der Waals mixing rules, 59
21 and the excess Gibbs energy mixing rules. van der 60
22 Waals mixing rules use the composition and mix- 61
23 ing parameters, which are fitted to experimental data, 62
24 to estimate the attractive and repulsive terms of the 63
25 cEoS. The excess Gibbs energy mixing rules inte- 64
26 grate activity coefficient models into the cEoS, thus 65
27 allowing for an improved estimation of the vapor- 66
28 liquid equilibrium properties, especially for polar flu- 67
29 ids. In order to extend the use of either of these mix- 68
30 ing models to new refrigerants, it is necessary to be 69
31 able to predict the mixing parameters or the activ- 70
32 ity coefficients based on a general knowledge of the 71
33 molecule. 72

34 The group contribution volume translated Peng 73
35 Robinson equation of state (GC-VTPR EoS) was first 74
36 proposed by Ahlers and Gmehling (2002a; 2002b) 75
37 with the aim of developing a universal, simple and 76
38 accurate way of estimating the thermophysical be- 77
39 havior of both polar and non-polar fluids. In its orig- 78

inal form, the GC-VTPR EoS combined the Twu-
alpha function for the attraction term (Twu et al.,
1995), the volume translation as proposed by P eneloux
et al. (1982), and the modified UNIFAC model (Fre-
denslund et al., 1975) for the mixing rule. In this
way, a general method was introduced to express the
interaction between the molecules in the mixture, based
only on a functional group contribution approach.
With this method, it was not necessary to fit the mix-
ing parameter for each possible molecule pair of newly
developed mixtures for which no experimental data
was available. Moreover, the volume translation pro-
vided a correction to the saturated liquid volume, which
is one of the weaknesses of cubic EoS. A similar ap-
proach was presented by Jaubert and Mutelet (2004),
who presented the PPR78 EoS as a combination of
the Peng-Robinson EoS with a group contribution
method for the estimation of the mixing parameters
using a van Laar type activity-coefficient model.

A number of works have been published on the
use of the GC-VTPR EoS, most of them focused on
the prediction of different mixtures of organic com-
pounds (e.g. alkanes, alcohols, acids) (Schmid and
Gmehling, 2016), showing good agreement with ex-
perimental results. However, the ability of the GC-
VTPR EoS to reproduce the properties of refrigerant
mixtures, including new halogenated olefins, has not
been studied so far. Only Qian et al. (2017) consid-
ered refrigerants in their extension of the work of the
PPR78 EoS to predict the mixing parameters of some
HFOs blends. Nevertheless, not all the functional
groups needed to define the refrigerants considered
in this work were defined in Qian et al. (2017), and
the considered mixing rule was the classical van der
Waals rule.

This work presents an assessment of the accuracy
of the GC-VTPR EoS to predict the saturation prop-
erties of a number of commercial refrigerant mix-
tures with low GWP and zero ozone depletion poten-

tial (ODP). The predictive capacity of the GC-VTPR EoS is analyzed over different pressure and temperature ranges, and is compared with that of the conventional Peng-Robinson equation of state (PR EoS), the translated Peng-Robinson equation of state (PR+ EoS), and a multi-parameter Helmholtz-energy-explicit EoS (HEOS). The objectives of this work are:

- To quantify the accuracy of the GC-VTPR EoS when predicting the saturated pressures and saturated liquid and vapor densities of the selected refrigerant mixtures.
- To present the fitted values of the interaction parameters of the modified UNIFAC needed for the representation of a number of refrigerants in the GC-VTPR model.
- To provide the research and the industrial community with an assessment on the suitability of GC-VTPR EoS for the study of new refrigerant mixtures.
- To describe in detail the algorithm used for fitting the interaction parameters.

This work presents a number of novel contributions. First, the ability of the GC-VTPR EoS to predict the behavior of refrigerant mixtures containing the new low-GWP hydrofluoroolefins, dimethyl ether, hydrofluorocarbons, and hydrocarbons, was thoroughly evaluated. Second, the values of the group surface areas of the UNIFAC model that were missing for specific functional groups were fitted based on the complete dataset of available experimental data. Third, indications on the use of the GC-VTPR EoS for the studied mixtures, based on the analyzed relative deviations of the predictions for the evaluated properties, are given.

The outline of this paper is as follows: in Section 2, the GC-VTPR EoS is introduced. In Section 3 the binary mixtures analyzed in this work are selected based on their importance for the industry. Section 4 explains

the methods used to fit the parameters of the mixing model. Section 5 presents the results of the predictions of the GC-VTPR EoS for different properties, and selected mixtures. Concluding remarks are given in Section 6.

2. Thermodynamic Modeling

2.1. Cubic equations of state

An EoS relates a number of thermodynamic variables, defining the state of a substance so that any other thermodynamic property can be derived from it. A cEoS, normally expressed in a pressure-explicit form, gives the pressure of a fluid p as a function of the temperature T and molar volume v , and can be expressed as a polynomial of the third order in the molar volume. This type of equation is generally referred to as $p - v - T$ EoS and links the liquid and vapor phases with a single equation (Frey et al., 2007).

The first cubic equation of state was developed by van der Waals (1873), and is expressed as follows:

$$\left(p + \frac{a}{v^2}\right)(v - b) = RT \quad (1)$$

where the a and b parameters are functions of the critical pressure and critical temperature of the fluid, and R is the ideal gas constant. The parameter a is called the *attraction term*, and b is the *covolume* (or effective molecular volume) as they account, respectively, for the attraction and repulsion forces between the molecules of the fluid. One of the main advantages of this EoS, which is shared by many other cEoS, is that only the knowledge of the critical temperature T_c and critical pressure p_c are required to define the model; these properties are frequently tabulated in handbooks and databases for a large number of substances.

Since the publication of this first cEoS, a number of modifications have been applied to the model in order to improve its prediction ability (Valderrama, 2003; Wei and Sadus, 2000; Lopez-Echeverry et al., 2017). Most of these improvements modify the attraction term a and the repulsion term b and express

1 them as functions of other variables. One of the most 37
 2 important modifications consists of the addition of a
 3 temperature dependent function to the attractive term,
 4 the so-called alpha function. In this way, the pa-
 5 rameter a is generally expressed as a constant part
 6 a_c (a function only of tabulated critical parameters
 7 of the fluid) multiplied by a temperature dependent
 8 term $\alpha(T_r)$, where T_r is the reduced temperature $T_r =$
 9 T/T_c . Examples of equations applying a temperature-
 10 dependent attraction term are the Soave-Redlich-Kwong
 11 (SRK) EoS (Soave, 1972), and the Peng-Robinson
 12 (PR) EoS (Peng and Robinson, 1976).

13 2.1.1. Peng-Robinson equation of state 38

14 As described in Poling et al. (2001), the fam- 39
 15 ily tree of cEoS can be cast into a common struc- 40
 16 ture, where the different modifications of the attrac- 41
 17 tion term are tabulated with adjustable parameters. 42
 18 Bell and Jäger (2016) carried out a similar exercise, 43
 19 for the SRK EoS, PR EoS, and the van der Waals 44
 20 EoS, with the aim of expressing the analytic deriva- 45
 21 tives of these EoS in a form compatible with the multi- 46
 22 parameter Helmholtz-energy-explicit EoS. In this frame-
 23 work, the cEoS is expressed in the following form: 48

$$p = \frac{RT}{v-b} - \frac{a(T)}{(v+\Delta_1 b)(v+\Delta_2 b)} \quad (2) \quad 49$$

24 where Δ_1 and Δ_2 are different for each EoS, being
 25 $\Delta_1 = 1 + \sqrt{2}$ and $\Delta_2 = 1 - \sqrt{2}$ for the PR EoS.
 26 The PR EoS is a modification of the SRK EoS that
 27 allows for better predictions of molar volumes in the
 28 liquid region and a better representation of the vapor-
 29 liquid equilibrium for many mixtures (Valderrama,
 30 2003). These features have made the PR EoS into
 31 one of the most used cEoS today. Although other
 32 cEoS have been developed, none has demonstrated a
 33 clear general advantage in thermodynamic property
 34 predictions (Frey et al., 2007).

35 The PR EoS for a pure fluid, expressed explicitly
 36 in terms of pressure, has the following form:

$$p = \frac{RT}{v-b} - \frac{a_c \alpha(T_r, \omega)}{v(v+b) + b(v-b)} \quad (3) \quad 58$$

where the parameters are expressed as follows:

$$a_c = 0.45724 \left(\frac{R^2 T_c^2}{p_c} \right) \quad (4)$$

$$b = 0.07780 \left(\frac{RT_c}{p_c} \right) \quad (5)$$

$$\alpha(T_r, \omega) = \left[1 + m(\omega) (1 - \sqrt{T_r}) \right]^2 \quad (6)$$

where the term m is a function of the acentric factor
 and is given as follows (for $\omega \leq 0.491$):

$$m(\omega) = 0.37464 + 1.54226\omega - 0.26992\omega^2. \quad (7)$$

For $\omega > 0.491$, the alternative form in Peng and
 Robinson (1976) is recommended.

The parameters a_c and b as defined here are fluid
 dependent. In the case of fluid mixtures, a mixing
 rule is necessary. See the work by Valderrama (2003)
 for a list of common mixing rules. The classical mix-
 ing rule is that of van der Waals, which can be aug-
 mented by one (k_{ij}) or two (k_{ij} and l_{ij}) adjust-
 able parameters. These parameters need to be fitted to ex-
 perimental data for each fluid pair. In the scope of
 this work, the van der Waals mixing rule without ad-
 justable parameters (equivalent to $k_{ij} = 0$ and $l_{ij} = 0$)
 is used for the Peng-Robinson (PR) model:

$$a_c = \sum_i \sum_j x_i x_j a_{ij}; \quad a_{ij} = \sqrt{a_{c,i} a_{c,j}} \quad (8)$$

$$b = \sum_i \sum_j x_i x_j b_{ij}; \quad b_{ij} = \frac{b_i + b_j}{2} \quad (9)$$

51 2.2. Volume translation

52 As mentioned in the previous section, cEoS gen-
 53 erally yield poor predictions of liquid phase densi-
 54 ties. For instance, the conventional PR EoS yields
 55 errors of more than 17% in the prediction of the den-
 56 sity of ordinary water at 298 K and 1 bar. A standard
 57 approach to address this problem is to apply a correc-
 58 tion to the liquid volume, which has nearly no impact
 1 on the gas region volumes.

The correction (or translation) term c , which is applied as in $v_{\text{corr}} = v_{\text{EoS}} + c$ equals the difference between the predicted and experimental saturated liquid molar volumes at the reduced temperature $T_r = 0.7$ (Schmid and Gmehling, 2012) as:

$$c = \left(v_{\text{exp}} - v_{\text{cEoS}} \right) \Big|_{T_r=0.7}. \quad (10)$$

Based on this term, the volume translated Peng-Robinson equation of state (PR+ EoS) can be rewritten as:

$$P = \frac{RT}{v + c - b} - \frac{a_c \alpha(T_r, \omega)}{(v + c)(v + c + b) + b(v + c - b)}. \quad (11)$$

This approach yields good results, although temperature dependent volume translations could also be used in order to enhance the accuracy near the critical point, or for specific fluids (Ji and Lempe, 1997). The work of Jaubert et al. (2016) and Privat et al. (2016) investigates the impact of volume translation on the other thermodynamic properties that can be obtained from an equation of state.

2.3. The group contribution volume translated Peng-Robinson equation of state

The modification of the PR EoS proposed by Ahlers and Gmehling(2002a; 2002b) consists of a combination of several of the above mentioned improvements, with the aim of developing a universal, accurate model for the prediction of thermophysical properties of fluids. This modification is, in fact a group contribution volume translated version of the PR EoS, and will be referred to as GC-VTPR EoS in this manuscript for simplicity.

As explained in the previous section, this new EoS applies a constant translation to the molar volume to improve the accuracy of the predictions in the liquid region. Moreover, the attraction term used is the one presented by Twu et al. (1991), which is expressed as follows:

$$\alpha(T_r, \omega) = T_r^{N(M-1)} \exp \left[L \left(1 - T_r^{MN} \right) \right], \quad (12)$$

where the parameters L , M and N have to be fit experimentally for each pure substance. The values of these parameters for the fluids considered in this work can be found in Appendix A. Although the use of the Mathias-Copeman alpha function (Mathias and Copeman, 1983) could be also a possibility, the consistency checks of Le Guennec *et al.* (2016a) suggest that the Twu alpha function should be preferred.

Finally, the group contribution part of the EoS comes from the use of the UNIFAC group contribution method to predict the activity coefficients of the excess Gibbs energy mixing rule. In this sense, while a simple arithmetic mixing rule is used for the covolume b , as shown in Eqs. 13 and 14, a mixing rule, which is based on the Gibbs energy, is used for the attractive term a as in Eq. (15) (Schmid and Gmehling, 2012; Chen et al., 2002):

$$b = \sum_i \sum_j x_i x_j b_{ij} \quad (13)$$

$$b_{ij} = \left(\frac{b_{ii}^{\frac{3}{4}} + b_{jj}^{\frac{3}{4}}}{2} \right)^{\frac{4}{3}} \quad (14)$$

$$a(T_r, \omega) = b \sum_i x_i \frac{a_{ii}}{b_{ii}} + \frac{g^{E,R}}{-0.53087 \text{ J mol}^{-1}}. \quad (15)$$

The prediction of the residual part of the Gibbs energy $g^{E,R}$ by a group contribution approach will be further discussed in detail in the next section. To conclude, the mixing rule used for the volume translation parameter c is given as follows:

$$c = \sum_i x_i c_i. \quad (16)$$

2.3.1. The Universal Quasichemical Functional Group Activity Coefficients

The residual part of the excess Gibbs energy from Eq. (15) is defined through the activity coefficients as follows:

$$g^{E,R} = RT \sum_i x_i \ln \gamma_i^R, \quad (17)$$

Here $g^{E,R}$ represents the excess molar Gibbs energy and γ_i^R is the residual part of the activity coefficient of component i . The universal functional activity coefficient (UNIFAC) is a semiempirical method that predicts activity coefficients of fluids, based on their molecular structure, by using contributions for each of the interactions between pairs of structural groups in non-electrolyte systems, which are fitted to experimental data (Poling et al., 2001). The UNIFAC group contribution model was developed to predict the vapor-liquid equilibrium of mixtures, by considering them as mixtures of structural groups, instead of mixtures of components. This approach led to a general formulation that allowed the estimation of the vapor-liquid equilibrium of most of the systems of commercial interest.

The value of the activity coefficient of a given component in a mixture can be decomposed into a combinatorial and a residual part as in Eq. 18 (Poling et al., 2001):

$$\ln \gamma_i = \ln \gamma_i^C + \ln \gamma_i^R \quad (18)$$

The combinatorial part is defined as:

$$\ln \gamma_i^C = \ln \frac{\phi_i}{x_i} + \frac{z}{2} q_i \ln \frac{\theta_i}{\phi_i} + l_i - \frac{\phi_i}{x_i} \sum_j x_j l_j \quad (19)$$

$$l_i = \frac{z}{2} (r_i - q_i) - (r_i - 1). \quad (20)$$

Here x_i is the molar fraction of the component i , z refers to the coordination number (usually equal to 10), ϕ_i is the segment fraction, θ_i is the area fraction, r_i is the molecular van der Waals volume, and q_i is the molecular surface area. Each of the last four

variables are defined as follows:

$$\theta_i = \frac{q_i x_i}{\sum_j q_j x_j} \quad (21)$$

$$\phi_i = \frac{r_i x_i}{\sum_j r_j x_j} \quad (22)$$

$$r_i = \sum_k v_k^{(i)} R_k \quad (23)$$

$$q_i = \sum_k v_k^{(i)} Q_k, \quad (24)$$

where $v_k^{(i)}$ is the number of groups of type k in molecule i . The van der Waals volume R_k and surface area Q_k are tabulated for a wide range of structural groups in Poling et al. (2001, Table 8.23).

The residual part of the activity coefficient is expressed as:

$$\ln \gamma_i^R = \sum_k v_k^{(i)} (\ln \Gamma_k - \ln \Gamma_k^{(i)}) \quad (25)$$

where Γ_k is the residual activity coefficient of group k , and $\Gamma_k^{(i)}$ is the pure fluid group residual activity coefficient of group k (the residual activity coefficient of group k in a reference solution containing only molecules of type i). These residuals can be obtained from Eq. (28), as:

$$\ln \Gamma_k = Q_k \left[1 - \ln \left(\sum_m \theta_m \psi_{mk} \right) - \sum_m \frac{\theta_m \psi_{mk}}{\sum_n \theta_n \psi_{nm}} \right] \quad (26)$$

$$\theta_m = \frac{Q_m X_m}{\sum_n Q_n X_n} \quad (27)$$

$$\psi_{mn} = \exp \left(-\frac{a_{mn} + b_{mn} T + c_{mn} T^2}{T} \right), \quad (28)$$

Here θ_m is the area fraction of group m , ψ_{mn} is the group interaction parameter, X_m is the mole fraction of the group m in the mixture, and a_{mn} , b_{mn} and c_{mn} are group interaction parameters obtained by fitting experimental data and are tabulated in databases.

3. Selected mixtures

The Air-Conditioning, Heating, and Refrigeration Institute (AHRI) has recently identified a number of mixtures of hydrofluorocarbons (HFCs) and hydrofluoroolefins (HFO) to replace the HFCs with high GWP that are currently in use (e.g., R-134a, R-404A, R-410A¹). These proposed mixtures contain at least two of the following pure refrigerants: R-32, R-125, R-134a, R-152a, R-1234yf, *n*-butane, isobutane, and dimethyl ether. Following this recommendation, several commercial mixtures containing these components are available in the market (Mota-Babloni et al., 2015):

- R-134a + R-1234yf: D-4Y, XP-10
- R-32 + R-1234yf: D2Y60, DR-5

Several commercial refrigerant families such as R-407 (R-32/R-125/R-134a), R-417 (R-125/R-134a/*n*-butane), R-422 (R-125/R-134a/isobutane), and R-451 (R-1234yf/R-134a) are relevant for refrigeration and heat pump applications. Moreover, the use of hydrocarbons as refrigerants is regaining interest as they comply with the recent environmental regulations on GWP, while having a low cost, though they do introduce some flammability concerns. The flammable compound dimethyl ether (DME) has also been proposed as an alternative refrigerant given its good heat transfer properties, high availability and low GWP (Ben Adamson and Airah, 1998).

In this work, we selected a set of binary mixtures for the evaluation of the performance of the GC-VTPR EoS based on the aforementioned recommendations, and on the availability of experimental data. The selected mixtures are summarized in Table 1, and comprise a set of binary mixtures containing the above mentioned components, with variable compositions.

¹The refrigerant nomenclature used in this work corresponds to the ASHRAE 34 standard (ASHRAE, 2016); the ISO 817 standard ISO 817:2014 (en) is substantially similar.

Table 1: Binary refrigerant mixtures included in this work. In each cell, the numerator is the number of experimental vapor-liquid equilibrium data points (PTXY or bubble-point pressure or dew-point pressure) and the denominator gives in parentheses the numbers of saturated liquid and vapor density experimental data points, respectively.

isobutane	$\frac{64}{(0,0)}$					
<i>n</i> -butane	$\frac{181}{(11,0)}$	$\frac{132}{(4,0)}$				
R-1234yf	0	$\frac{60}{(0,0)}$	$\frac{0}{(0,0)}$			
R-125	$\frac{121}{(0,0)}$	$\frac{140}{(0,0)}$	$\frac{64}{(0,0)}$	$\frac{84}{(0,0)}$		
R-134a	$\frac{92}{(0,0)}$	$\frac{60}{(0,0)}$	$\frac{138}{(0,0)}$	$\frac{63}{(0,0)}$	$\frac{417}{(79,28)}$	
R-32	$\frac{132}{(0,0)}$	$\frac{75}{(0,0)}$	$\frac{182}{(0,0)}$	$\frac{132}{(18,22)}$	$\frac{673}{(97,101)}$	$\frac{794}{(127,28)}$
R-143a	$\frac{64}{(0,0)}$	$\frac{20}{(0,0)}$	$\frac{134}{(0,0)}$	$\frac{45}{(0,0)}$	$\frac{196}{(108,42)}$	$\frac{225}{(0,0)}$
	DME	isobutane	<i>n</i> -butane	R-1234yf	R-125	R-134a
						R-32

3.1. Experimental database

Data provided via the NIST ThermoData Engine #103b version 10.1 were used in this work for the evaluation of the performance of the GC-VTPR EoS. The database contains experimental data of pure fluids and mixtures collected from publications. Three main data sets were used in this work:

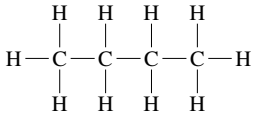
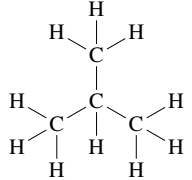
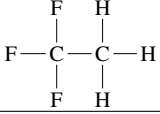
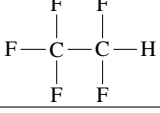
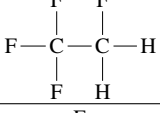
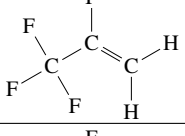
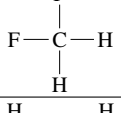
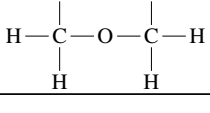
- Vapor-liquid equilibrium data containing the pressure, temperature, and molar fraction of the components for bubble and/or dew points.
- Density data containing the specific volume, pressure, temperature, and molar fraction in the liquid and/or gas phase, as well as for bubble and/or dew points.
- Pure fluid saturated liquid density data, for the computation of the volume translation term c of Eq. (16).

4. Parameter fitting for the GC-VTPR EoS

In order to estimate the activity coefficients for each selected mixture according to Eqs. (18) to (28), it is first necessary to decompose each of the components into structural groups that are covered by the database of group parameters. In this work, the group decomposition was inspired by the groups defined by Gmehling (1985), for which the revised and

59 updated UNIFAC parameters are available. The re- 4
 60 frigerant R-32 could not be decomposed through the 5
 61 use of the available groups, and was therefore given 6
 62 its own group. The group decompositions of the con- 7
 63 sidered fluids are described in Table 2, and once spec- 8
 64 ified, were not changed.

Table 2: Molecules and secondary group decomposition of the 10
 components of the studied mixtures, derived from the group 11
 decompositions of Gmehling (1985). The group indices corre- 12
 spond to the subgroup indices sgi and are defined in Table 3. 13

Component	Formula	Molecule	Secondary groups $\sum_i \text{count}_i \cdot sgi_i$
<i>n</i> -butane	C ₄ H ₁₀		2 · (1) + 2 · (2)
isobutane	C ₄ H ₁₀		3 · (1) + 1 · (3)
R-143a	C ₂ F ₃ H ₃		1 · (4) + 1 · (1)
R-125	C ₂ F ₅ H		1 · (4) + 1 · (5)
R-134a	C ₂ F ₄ H ₂		1 · (4) + 1 · (6)
R-1234yf	C ₃ F ₄ H ₂		1 · (4) + 1 · (8)
R-32	CF ₂ H ₂		1 · (7)
DME	C ₂ H ₆ O		1 · (1) + 1 · (9)

65 The group normalized surface area Q_k for each
 66 of the k groups can in theory be calculated by *ab*
 1 *initio* approaches in which an isosurface of the elec-
 2 tron density distribution is used to define the surface
 3 area of a group. This exercise only yields approx-

imate values for the surface area of a group due to
 the impact of the intramolecular group-group inter-
 actions. Nonetheless, the surface areas obtained by
 this method are theoretically based, and as such, are
 constrained to yield a self-consistent formulation for
 the group surface areas. In our study we obtained
 initial guesses for the group surface area from the
 group surface areas given in Poling *et al.*(2001). The
 values we used are in Table 3. For the groups that
 are not in Poling *et al.* ($-HCF_2$, $-CFH_2$, CF_2H_2 ,
 and $-CF=CH_2$), the group surface areas were calcu-
 lated by an additive scheme as detailed in the sup-
 plemental material that was based on the numerical
 values of group surface areas of Bondi (1968). This
 method provides the values of the van der Waals sur-
 face areas of the groups in cm^2/mol , which are con-
 verted to normalized surface areas Q_k by dividing by
 the surface area of a standard segment (a methylene
 group in polymethylene) given as 2.5×10^9 cm^2/mol
 (Abrams and Prausnitz, 1975, Appendix B). Previous
 works (Schmid and Gmehling, 2012, 2016; Schmid
 et al., 2014) suggest that the best approach to de-
 termine the group surface areas is empirical fitting,
 but we did not follow that recommendation because
 some of the Q_k values obtained with empirical fitting
 can be non-physical if not properly constrained.

4.1. Fitting algorithm

In the fitting campaign, only vapor-liquid equi-
 librium data for which the composition of both of the
 co-existing phases were known were considered. For
 phases in equilibrium, the chemical potential of all
 components in all phases must be equal. The equal-
 ity of chemical potentials can be expressed as:

$$\mu'_i(T, p, \vec{x}') = \mu''_i(T, p, \vec{x}''), \quad (29)$$

where μ'_i and μ''_i are the chemical potentials of species
 i in the saturated liquid and vapor, respectively, and
 \vec{x}' and \vec{x}'' are the compositions of the liquid and va-
 por phases, respectively. This equality can be shown
 (Kunz et al., 2007, pp. 58-59) to be equal to the
 equality of fugacity coefficients times their respec-

tive mole fraction, as:

$$x'_i \varphi'_i(T, p, \vec{x}') = x''_i \varphi''_i(T, p, \vec{x}'') \quad (30)$$

which is equivalent (from $f_i = x_i p \varphi_i$) to the fugacities of all components in all phases being equal, as:

$$f'_i(T, p, \vec{x}') = f''_i(T, p, \vec{x}''). \quad (31)$$

The goal of the optimizer is then to best satisfy the phase equilibrium conditions for all of the experimental data points by adjusting the group surface areas and interaction parameters. For the k -th experimental data point, we have the expense contribution as follows:

$$e_k^2 = \sum_{i=0}^1 \left[\ln \varphi'_i(T, p, \vec{x}') - \ln \varphi''_i(T, p, \vec{x}'') - \ln \left(\frac{\vec{x}'_i}{\vec{x}''_i} \right) \right]^2. \quad (32)$$

The cost function to be minimized by modifying the group-group interaction parameters is the summation of the weighted expense contributions as:

$$\text{COST}(\vec{a}_{ij}, \vec{a}_{ji}) = \sum_k w_k e_k \quad (33)$$

The optimization of the adjustable parameters is carried out as a global optimization problem. The research domain of global optimization is vast, spanning several fields of study. Our experiments showed that the quality of the parameter values obtained is quite sensitive to the precise method of optimization employed. After experimenting with several optimization approaches, we settled on the use of differential evolution (Storn and Price, 1997), one of the global optimization techniques that has found the broadest application. This stochastic optimization methodology can be readily understood and implemented in only a handful of lines of code. In differential evolution, the initial domains of each of the adjustable parameters must be specified. The bounds on the interaction parameters a_{ij} and a_{ji} were set to $[-1000, 1000]$ for each variable. The parameters b_{ij} , b_{ji} , c_{ij} , and c_{ji} were not fit because doing so dramati-

ically increased the challenge of the optimization, without a straightforward uniform improvement of the model. The weights on the data sets were determined to balance the weight per binary pair; per-binary-pair weights were set such that each binary pair contributed to the cost function and systems with extensive data (e.g., R-32 + R-125) did not totally dominate the cost function. Table B.5 in Appendix B collects the values of the interaction parameters a_{mn} of Eq. (28).

Table 3: Group surface areas for each group. The values in normal font were directly obtained from Poling et al. (2001) and the values in bold font were obtained from the additive scheme detailed in the supplemental material based on the work of Bondi (1968).

Group number		Formula	UNIFAC
Main	Subgroup		Q [-]
1	1	-CH ₃	0.848
	2	-CH ₂ -	0.540
	3	-CH<	0.228
2	4	-CF ₃	1.380
	5	-HCF ₂	1.108
	6	-CFH ₂	0.980
3	7	CF ₂ H ₂	1.420
4	8	-CF=CH ₂	1.428
5	9	-OCH ₃	1.088

5. Results

In this section, the performance of the GC-VTPR EoS is compared to experimental data and to other equations of state. These comparison EoS are the reference multi-fluid equation of state, as implemented in NIST REFPROP (Lemmon et al., 2018) library and the Peng-Robinson EoS without volume translation. For the PR EoS, the implementation of CoolProp (Bell et al., 2014) is used. This analysis allows for a comparison of the performance of the GC-VTPR EoS with that of the most accurate mixture models available in the literature. The comparison

presented in this section is performed in terms of relative deviations from the experimental data. The percentage relative deviation of an EoS prediction of a parameter χ with respect to the experimental value is defined as follows:

$$RD = 100 \times \left(\frac{\chi_{\text{calc}} - \chi_{\text{exp}}}{\chi_{\text{exp}}} \right) \quad (34)$$

The results in this section begin with a discussion of the fidelity of the model to the experimental vapor-liquid equilibrium data of the mixture. As described in the literature (Jaubert et al., 2016; Privat et al., 2016) and as discussed above, the addition of P eneloux-style volume translation does not shift the phase equilibrium, and therefore, the effects of the GC-VTPR model on the VLE data representation can be considered in two parts: i) the impact of the fitted parameters on the representation of the VLE data ii) the volume-translated VLE data for the equilibrium phase densities.

All the figures depicting the percentage RD for the different properties and for all the studied mixtures are available in the Supporting Information. In the following sections, only the most representative figures for each case are shown. These figures are classified into three types depending on the way RD are depicted, and are explained below:

- *Violin plots*: the distribution of the deviation in a similar manner to a histogram. The lower and upper bars represent the minimal and maximal values, respectively. The middle bar represents the median.
- *Composition dependency plots*: the relative deviation versus the molar fraction of the first component of the mixture, which allows for an assessment of how the composition affects the accuracy of the EoS mixing rule.
- *Temperature dependency plots*: they represent the influence of temperature on the RD, in order to show potential temperature effects on the accuracy of the EoS.

5.1. Vapor-Liquid Equilibrium

Figure 1 and Fig. 2 present the pressure-composition isotherms for the mixtures R-125 + R-134a and isobutane + R-134a, respectively, as illustrative cases. Additional results for all the binary mixtures considered are available in the Supporting Information. The predicted values of the bubble and dew pressures for the mixture R-125 + R-134a are in good agreement with the available experimental values over the entire temperature range. However, a different behavior can be observed for the mixture isobutane + R-134a. This mixture was chosen as a representative of the predictive performance of the GC-VTPR EoS, as it presents azeotropic behavior at low molar fractions of isobutane. As it can be seen, while the predicted values at high temperatures match reasonably well the experimental bubble point data, the calculated values at low temperatures underestimate the bubble point pressure near the azeotrope.

The strength of the thermodynamic correction that the excess Gibbs energy contribution must provide is highly dependent on the similarity of the components forming the binary mixture and whether the mixture is likely to form azeotropes. In the case of *n*-butane + isobutane, for instance, all groups in the mixture are in the first ($m_{gi}=1$) main group, and therefore, the excess Gibbs contribution g^E is by definition zero. On the other hand, for binary mixtures that have cross-main-group binary interactions (isobutane + R-134a), the excess Gibbs energy contribution shifts the mixture thermodynamics. Figure 2 demonstrates that the model is able to capture strong positive-pressure azeotropes (which occur frequently in binary mixtures of refrigerant-like fluids).

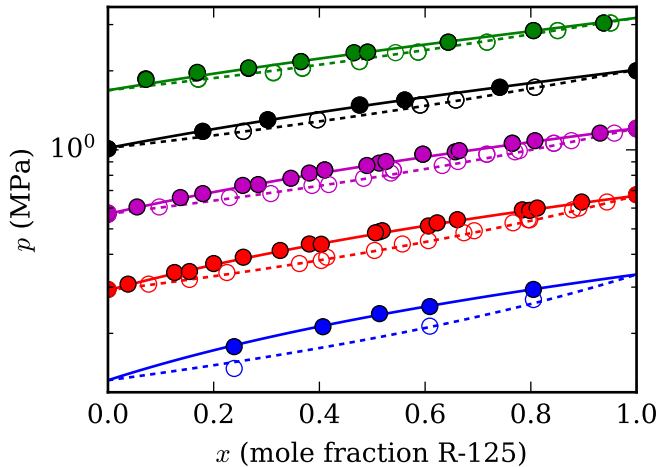


Figure 1: Selected pressure-composition isotherms (253.1, 273.1, 293.1, 313.1, 333.1 K) for the mixture R-125 + R-134a versus the mole fraction of R-125 with the GC-VTPR model in this work: ● bubble point experimental data; ○ dew point experimental data; — calculated bubble point; - - - calculated dew point. Experimental data points are taken from the literature (Kleemiss, 1997; Kato and Nishiumi, 2006; Higuchi and Higashi, 1995; Benmansour and Richon, 1999; Widiatmo et al., 1997; Nagel and Bier, 1995; Holcomb et al., 1998; Higashi, 1999a; Kobayashi and Nishiumi, 1998; Kim and Park, 1999; Nishiumi and Ohno, 2000)

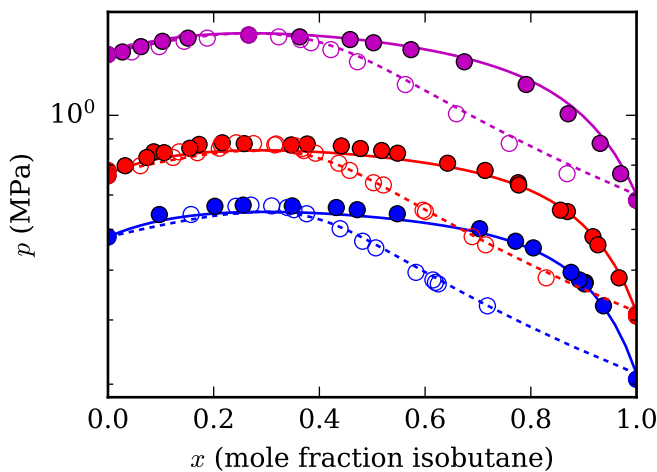


Figure 2: Selected pressure-composition isotherms (293.66, 303.2, 323.2 K) for the mixture isobutane + R-134a versus the mole fraction of isobutane with the GC-VTPR model in this work: ● experimental bubble point; ○ experimental dew point; — calculated bubble point; - - - calculated dew point. Experimental data points are taken from the literature (Lim et al., 2000; Bobbo et al., 1998)

Any *PTXY* experimental VLE measurement for which the compositions of both of the co-existing phases, temperature, and pressure are known can be

also be considered as two separate measurements, one for which the mixture is at the bubble-point (the liquid mixture at the bulk composition is in equilibrium with the incipient vapor phase), and another at the dew point (the gaseous mixture at the bulk composition is in equilibrium with the incipient liquid phase). Therefore, although the fitting campaign considered only *PTXY* data, the analysis of the mixture models considers bubble point and dew point data individually. Here we consider the binary mixture of DME + *n*-butane as an illustrative case of the analysis of the phase equilibrium pressures. We compare the model predictions of phase equilibrium pressure with those of Peng-Robinson, and the reference multiparameter model implemented in the industry standard NIST REFPROP library (Lemmon et al., 2018).

Although deviations in pressure are commonly presented in the literature (and will be here also), the deviation in phase equilibrium pressure is an imperfect metric to capture the “goodness” of the model. This is because as the VLE isotherms become very steep ($|dp/dx|$ becomes large along the VLE isotherm), it is no longer relevant to talk about deviations in pressure; it is better to talk about the orthogonal distance of the experimental data point from the VLE isotherm. Nonetheless, the deviation in pressure is an accessible metric for “quality-of-fit”, and particularly for mixtures with slender VLE “lenses”, pressure deviations are meaningful.

Figure 3 and Fig. 4 present the results for the mixture of isobutane + R-125; this is one of the mixtures with the largest worst-case relative deviations in saturation pressure (with some bubble-point pressure deviations greater than 30%). Figure 3 presents pressure-composition isotherms for the mixture isobutane + R-125 and in Fig. 4, the relative deviations for the bubble-point and dew-point pressures are shown for each of the EOS, as well as the composition and temperature dependence of the deviations of the models. One challenge with this mixture is that all the available *PTXY* data used to fit this mixture model were above 293 K, therefore the poor fidelity of this

63 model for temperatures below 293 K should not be
 64 considered as indictment of the general modeling ap-
 65 proach, rather a demonstration of the challenges to
 66 obtain the correct extrapolation behavior. For bubble-
 67 point pressures (left side of the figure), the mean ab-
 68 solute error for REFPROP is smallest in magnitude
 69 (2.8%), followed by GC-VTPR (9.2%) and Peng-
 1 Robinson (28.7%). The pure fluid endpoints at $x_1 =$
 2 0 and $x_1 = 1$ are governed by the behavior of the α
 3 function and the Twu parameters; for a pure fluid the
 4 UNIFAC contribution is zero.

5 At low temperatures, all of the mixture models
 6 deviate strongly from the experimental data. This
 7 can be partially explained by the data that were in-
 8 cluded in the fitting of the interaction parameters in
 9 NIST REFPROP. The binary interaction parameters
 10 fit for isobutane + R-125 in NIST REFPROP ($\beta_T=1.0$,
 11 $\gamma_T=0.90538$, $\beta_V=1.0$, $\gamma_V=1.0036$) were obtained in
 12 2002, and all of the experimental data at tempera- 1
 13 tures below 293 K were collected in 2007 in the pub- 2
 14 lication of Chen et al. (2007). This result highlights 3
 15 as well that although the mixture models in NIST 4
 16 REFPROP are in general the most accurate available 5
 17 in the literature, they are only as reliable as the exper- 6
 18 imental data that were available at the time the model 7
 19 was developed. The conventional Peng-Robinson EoS 8
 20 also demonstrates significant deviations from the ex- 9
 21 perimental data. For the dew-point pressures (right 10
 22 side of the figure), the mean error for REFPROP is 11
 23 smallest in magnitude (1.2 %), followed by GC-VTPR 2
 24 (4.0 %) and Peng-Robinson(18.2 %). Figure 3 shows 13
 25 a few of the isotherms, highlighting that the largest 14
 26 deviations are at low temperatures, below the range 15
 27 where the *PTXY* data needed for model fitting in this 16
 28 work are available.

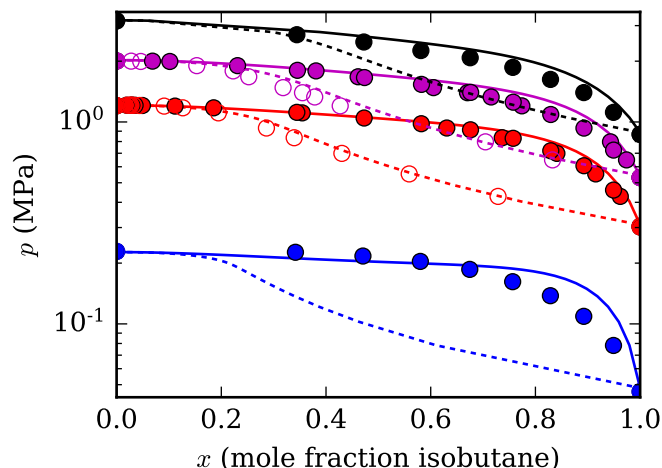


Figure 3: Selected pressure-composition isotherms (243.15, 293.15, 313.15, 333.15 K) for the mixture isobutane + R-125 versus the mole fraction of isobutane with the GC-VTPR model in this work: ● bubble point experimental data; ○ dew point experimental data; — calculated bubble point; - - - calculated dew point. Experimental data are from the literature (Chen et al., 2007; Lee et al., 2000)

17

Finally, in Fig. 5 we present an overview of the results from the modeling of the bubble-point pressure and the bubble-point density. In each entry in the matrix a violin plot is presented, showing the distribution of the error for the property for the given binary pair. One would like to see a flat “pancake” distribution centered around 0 % error. For many mixtures, the distribution is tightly clustered around zero. For other mixtures, a common systematic limitation of this fitting approach is seen: experimental *PTXY* data are available at higher pressures, and bubble-point pressure measurements are available at lower pressures. This is the case described above for isobutane + R-125. In general, where wide-ranging *PTXY* data were available for a given binary mixture, the model is able to represent the data faithfully. The bubble-point density deviations are described below.

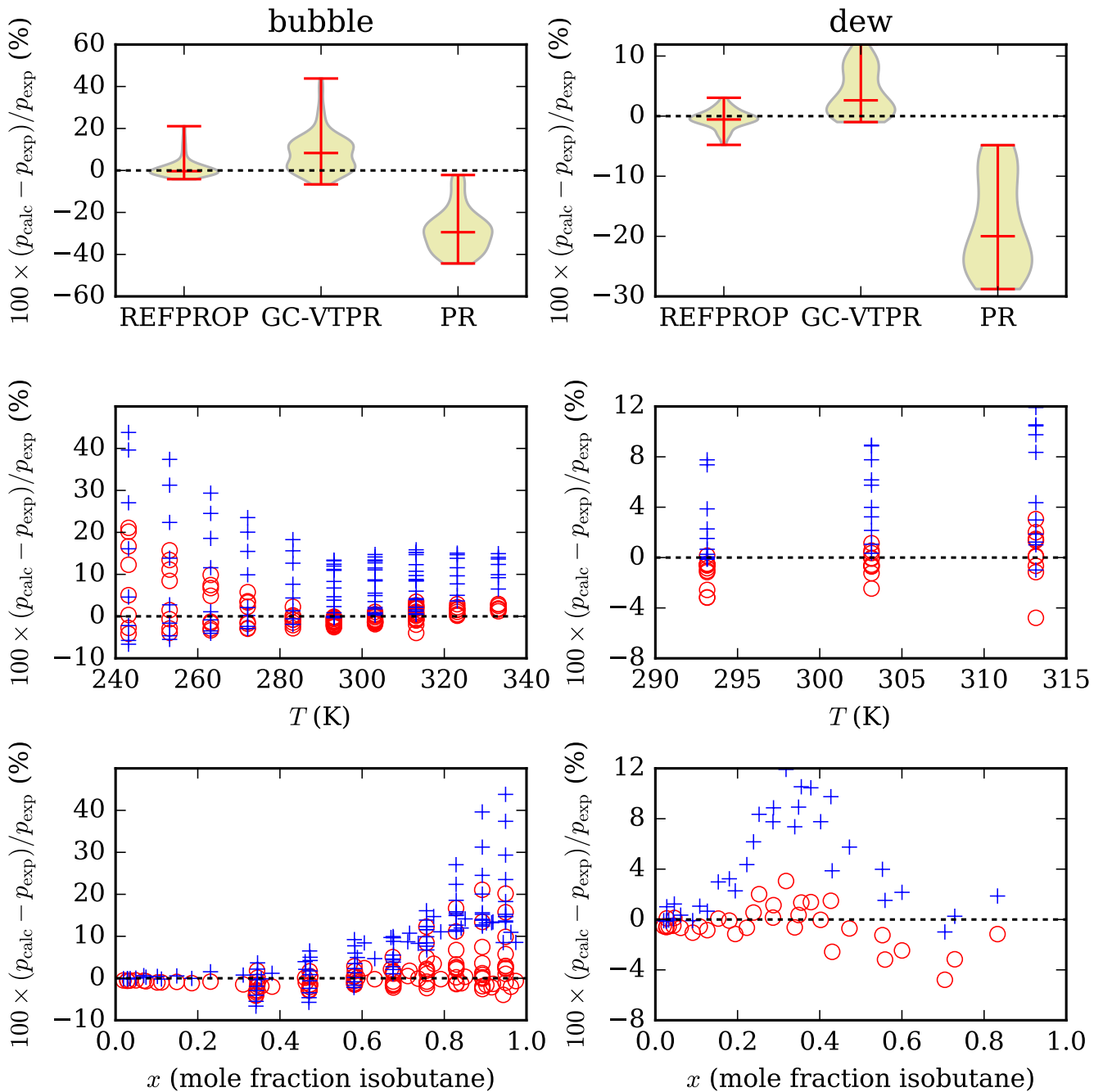


Figure 4: Deviation plots in saturation pressure for the mixture isobutane(1) + R-125(2) versus the mole fraction of isobutane and the temperature with the GC-VTPR model in this work. Experimental data are from the literature (Lee et al., 2000; Chen et al., 2007). Markers are given by \circ : REFPROP, $+$: GC-VTPR. The lower and upper bars in the violin plots represent the minimal and maximal values, respectively; the middle bar represents the median.

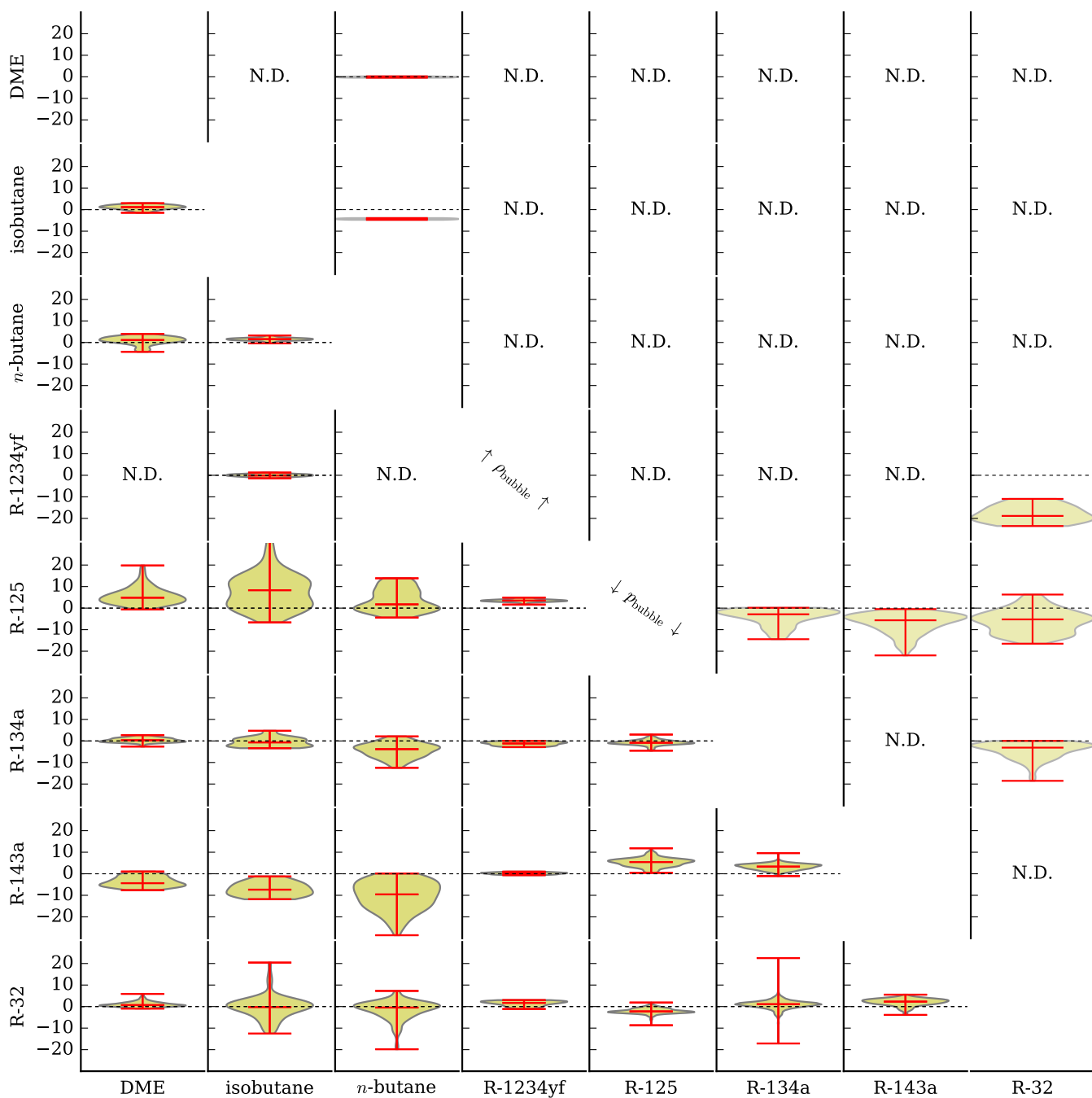


Figure 5: An overview of the goodness of fit for each binary pair, with violin plots shown for the deviations of bubble-point pressure and bubble-point density for the GC-VTPR model of this work as compared with the experimental data from the literature, as reported in ThermoDataEngine (details in the supplemental material). An entry of “N.D.” indicates that no experimental data are available for the mixture.

18 **5.2. Pure Fluid Saturated Liquid Densities**

19 The calculation of the volume translation parameter for the i -th component c_i , defined in Eq. (10),
 20 was extended to mixtures through the use of a linear
 21 mole fraction weighting rule, as indicated in Eq. (16).
 22 Experimental values of the saturated liquid density at
 23 exactly $T_r = 0.7$ are in general not available, there-
 24 fore the saturated liquid density at $T_r = 0.7$ was
 25 obtained through the use of a saturated liquid density
 26 ancillary equation, as in Outcalt and McLinden
 27 (1995), of the form $\rho_l = a_1 + a_2\tau^{\beta_1} + a_3\tau^{\beta_2} + a_4\tau^{\beta_3} +$
 28 $a_5\tau^{\beta_4} + a_6\tau^2 + a_7\tau^3 + a_8\tau^4$, where the coefficients $\beta_{1:3}$
 29 and $a_{1:8}$ were fitted to experimental liquid density
 30 data of the pure fluids. The translation term for each
 31 pure fluid c_i , was obtained by calculating the density
 32 at a reduced temperature of $T_r = T/T_c = 0.7$, as in
 33 $c_i = (v_{\text{calc}} - v_{\text{anc},i})|_{T_r=0.7}$.

34 Figure 6 shows the percentage relative deviations
 35 between the densities obtained with the fitted value
 36 of c_i for n -butane, and the experimental densities.
 37 The densities calculated by the non-volume-translated
 38 Peng-Robinson model are also shown for compari-
 39 son purposes. As expected, after applying volume
 40 translation, the deviations for the saturated liquid density
 41 at $T_r = 0.7$ is near zero. The deviations in sat-
 42 urated liquid density are less than 0.5% in the tem-
 43 perature range $0.6T_c$ to $0.8T_c$. Equivalent figures for
 44 the rest of the pure fluids can be found in the sup-
 45 porting material; the reduced specific densities and
 46 the volume translation terms c_i obtained through this
 47 process are also available in the supporting material.

49 **5.3. Mixture Saturated Liquid Densities**

50 In general, VLE density data for refrigerant mix-
 51 tures are much less common than bubble-point and
 52 dew-point pressure data. This scarcity is largely driven
 53 by the difficulty of carrying out phase equilibrium
 54 density measurements as compared with vapor-liquid
 55 equilibrium measurements. As a result, there are
 56 only seven binary mixtures with any bubble-point
 57 density measurements. Figure 5 shows the same kind
 58 of violin plots as were generated for the bubble-point
 59 pressure. There are many systems with no phase

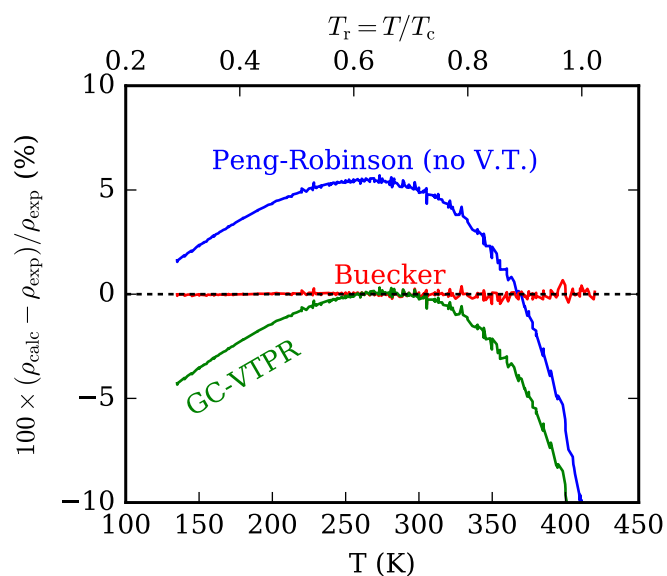


Figure 6: Relative deviations of the saturated liquid densities of n -butane from the multiparameter EOS of Buecker and Wagner (2006), GC-VTPR and PR compared with the experimental data from the literature (Dana et al., 1926; Coffin and Maass, 1928; Kay, 1940; Benoliel, 1941; Carney, 1942a,b; Legatski et al., 1942; Cragoe, 1943; Olds et al., 1944; Prengle et al., 1948; Klosek and McKinley, 1968; Sliwinski, 1969; Haynes and Hiza, 1976; McClune, 1976; Haynes and Hiza, 1977; Calado et al., 1978; Orrit and Laupretre, 1978; Thompson and Miller, 1980; Hsu et al., 1985; Kaminishi et al., 1988; Niesen, 1989; Vasserman et al., 1989; Holcomb et al., 1995; Kumagai and Takahashi, 1995; Dahlhoff et al., 2000; Glos et al., 2004; Kayukawa et al., 2005; Miyamoto and Uematsu, 2007).

60 equilibrium density measurements. In general, bubble-
61 point density measurements are carried out prior to
62 dew-point density measurements for a given mixture,
63 therefore there are only 5 systems for which *any* dew-
64 point density measurements are available. Only the
65 bubble-point density deviation plots are shown in this
66 figure.

1 The deviations in bubble-point density are in gen-
2 eral larger in relative terms than the deviations in
3 bubble-point pressure; this is a result of a number
4 of compounding errors. The first error contribution
5 arises from the UNIFAC contribution; if the UNIFAC
6 contribution shifts the phase equilibrium in a dele-
7 terious direction, the non-volume-translated equilib-
8 rium densities may also be perturbed. The volume
9 translation is then applied after the phase equilibrium
10 calculation, but as is evident in Fig. 6, the volume
11 translation has a rather small range in reduced tem-
12 perature where it is particularly effective. For state
13 points away from $T_r = 0.7$ for the pure fluids in the
14 mixture, the volume translation does not necessarily
15 compensate in the appropriate direction. The poor
16 matching of volume translation constants for pure
17 fluids in the mixture can be especially problematic
18 for mixtures where the critical temperatures of the
19 components are very different, although for the re-
20 frigerant mixtures studied in this work the critical
21 temperatures are relatively similar. The inclusion of
22 P eneloux-style volume translation does not always
23 improve the representation of liquid-phase densities,
24 and at low and high temperatures, the volume trans-
25 lation can significantly degrade the prediction of liquid-
26 like densities. On the other hand, much of the interest
27 for industrial applications is in the temperature range
28 near $0.7T_c$, so volume translation can be worthwhile
29 depending on the particulars of the modeling prob-
30 lem to be solved.

31 Figure 7 shows deviation plots for the bubble-
32 point densities for the mixture of R-143a + R-125.
33 This is a mixture with one of the worst representa-
34 tions of the bubble-point densities in Fig. 5, so it is
35 instructive to better understand this system. The pri-
36 mary reason for the poor representation of the phase

equilibrium densities is that the available densities
are not in the vicinity of $0.7T_c$ of the pure compo-
nents, the temperature at which the volume transla-
tion has been tuned. The deviations in bubble-point
density increase as the temperature increases away
from $0.7T_c$ of the pure components, while there is
minimal dependence on the composition of the mix-
ture. Other authors (Le Guennec et al., 2016b) also
note that away from the point at which the volume
translation has been tuned the representation of den-
sities is significantly worse.

6. Conclusions

In this work, the group contribution volume trans-
lated Peng Robinson equation of state (GC-VTPR
EoS) was applied to a set of constituent fluids form-
ing commercial refrigerant mixtures. The accuracy
of this equation of state was evaluated by analyzing
the relative deviations of the estimated values versus
experimental data of saturation pressures and satu-
rated liquid and vapor densities. The performance
of the GC-VTPR EoS was also compared to that of
the standard Peng-Robinson equation of state and the
multi-fluid Helmholtz energy equation of state im-
plemented in NIST REFPROP 10 (Lemmon et al., 2018).
This comparison allowed for an analysis of the po-
tential improvements in cubic equations of state through
the use of volume translation and an excess Gibbs en-
ergy group contribution term.

Based on the results of this analysis, the follow-
ing conclusions were drawn:

- The GC-VTPR EoS yields competitive accu-
racy with NIST REFPROP for the saturation
pressure of mixtures containing components with
similar molecular structure. As the difference
between the molecular structure of the com-
ponents increases, the GC-VTPR EoS tends to
yield larger deviations than REFPROP. This is
observed also for the Peng-Robinson EoS.
- The predicted liquid density values are strongly
influenced by the application of volume trans-

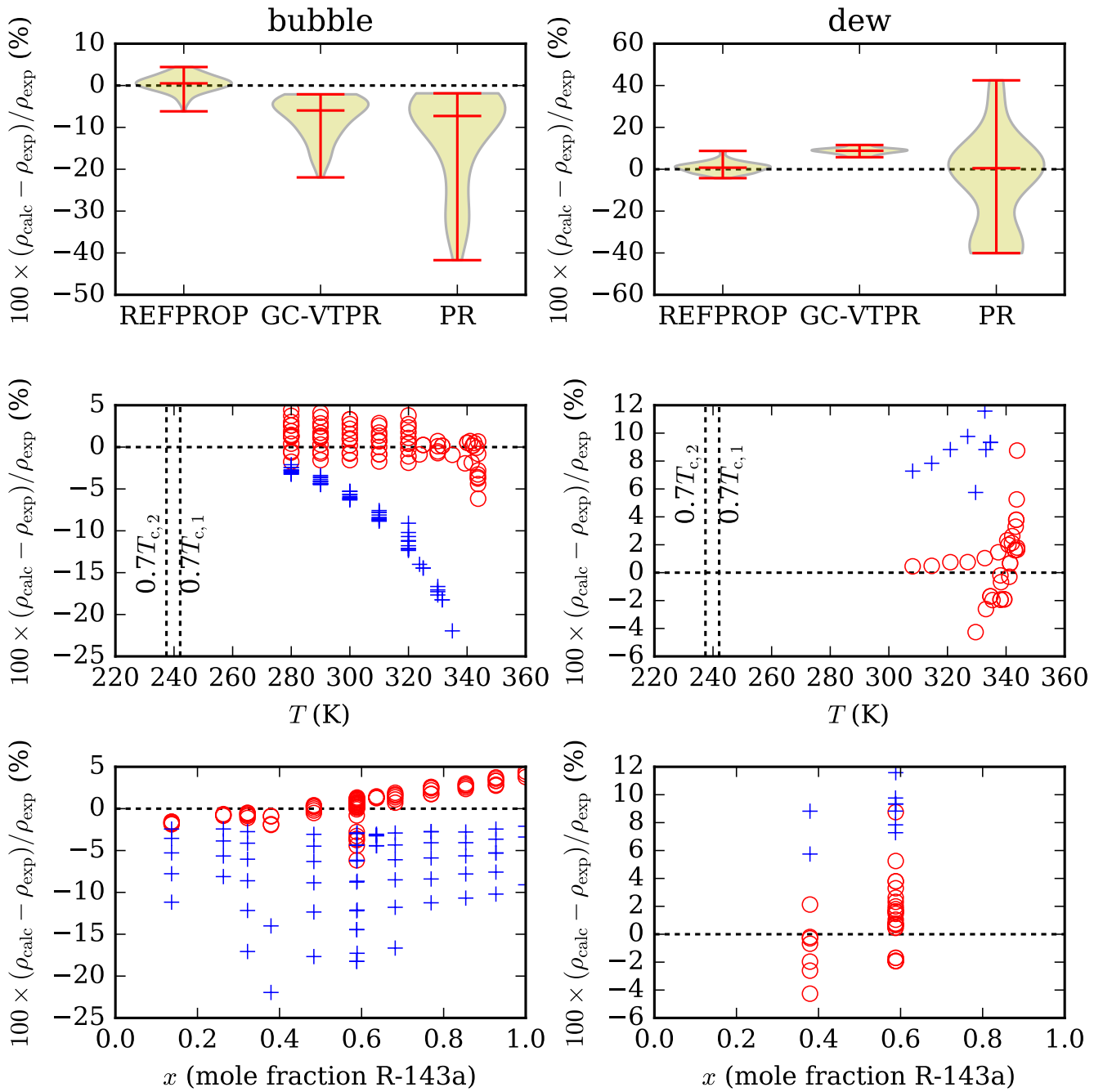


Figure 7: Deviation plots in saturation densities for the mixture R-143a (1) + R-125 (2) versus the mole fraction of R-143a and the temperature with the models investigated in this work. Markers are given by \circ : REFPROP, $+$: GC-VTPR. Experimental data points for which the vapor-liquid equilibrium calculations failed are not shown. The lower and upper bars in the violin plots represent the minimal and maximal values, respectively; the middle bar represents the median. Experimental data are from the literature (Ikeda and Higashi, 1995; Widiatmo et al., 1995; Fujimine et al., 1999; Higashi, 1999b; Kishizawa et al., 1999; Uchida et al., 1999).

lation; this is by design as the volume translation is intended to “repair” the saturated liquid densities. This volume translation parameter may benefit from a temperature dependence and an improved mixing rule that considers the size difference between the molecules.

- The GC-VTPR EoS evaluated in this work offers competitive results in terms of accuracy with other EoS and could be used for the study of new refrigerant mixtures for which insufficient experimental data are available to fit the highly accurate (and complicated) fluid models used in NIST REFPROP. Moreover, improvement of the volume translation and mixing rules provides opportunities to further improve the accuracy of this modeling framework.

7. Acknowledgements

The authors thank Jorrit Wronski (IPU) for coding support, Jens Abildskov (DTU) for the discussions on the fitting of activity coefficients. Jonathan Welliquet thanks the Erasmus+ project who provided financial support for his internship at DTU. Maria E. Mondejar acknowledges the financial support from the European Union’s Horizon 2020 research and innovation programme with a Marie Skłodowska-Curie Fellowship under grant agreement No 704201 with the project NanoORC (www.nanoorc.mek.dtu.dk).

Appendix A. Parameters for the Twu α function

The parameters L , M and N for the Twu α function (see Eq. 12) were optimized and tabulated by Bell et al. (2018) for 2570 fluids. Table A.4 presents the values of the parameters used in this work.

Appendix B. Interaction parameters for the term

$$a_{mn}.$$

The interaction parameters a_{mn} for Eq. (28) are collected in Table B.5. The parameters for a_{45} and a_{54} are unknown (and set to zero) because these groups

Table A.4: Consistent coefficients for the Twu α function for the fluids considered in this work. All coefficients have been taken from the work of Bell et al. (2018)

Fluid	L	M	N
<i>n</i> -butane	0.4652	0.8475	1.2010
isobutane	1.1121	0.9991	0.5440
R-143a	0.2450	0.8491	2.1298
R-125	1.0845	0.9986	0.7413
R-134a	0.3064	0.8298	2.0112
R-1234yf	0.1659	0.8437	2.6526
R-32	0.3436	0.8546	1.7906
DME	0.8312	0.8881	0.7446

were not present in any of the experimental data included in this study.

Table B.5: Interaction parameters a_{mn} in K.

mg	n=1	2	3	4	5
m = 1	0	197.06	268.17	69.746	17.476
2	2.2679	0	-9.3253	-96.001	-330.51
3	75.107	29.518	0	83.803	-78.799
4	-4.7829	269.44	206.02	0	0
5	540.81	999.99	35.719	0	0

References

- Abrams, D. S., Prausnitz, J. M., 1975. Statistical Thermodynamics of Liquid Mixtures: A New Expression for the Excess Gibbs Energy of Partly or Completely Miscible Systems. *AIChE J.* 21 (1), 116–128.
- Ahlers, J., Gmehling, J., 2002a. Development of a universal group contribution equation of state. 2. Prediction of vapor-liquid equilibria for asymmetric systems. *Ind. Eng. Chem. Res.* 41 (14), 3489–3498.
- Ahlers, J., Gmehling, J., 2002b. Development of a universal group contribution equation of state III. Prediction of vapor-liquid equilibria, excess enthalpies, and activity coefficients at infinite dilution with the VTPR model. *Ind. Eng. Chem. Res.* 41 (23), 5890–5899.
- ASHRAE, 2016. ANSI/ASHRAE Standard 34-2016 Designation and Safety Classification of Refrigerants.
- Bell, I. H., Jäger, A., 2016. Helmholtz Energy Transformations of Common Cubic Equations of State for Use with Pure Fluids and Mixtures. *J. Res. Nat. Inst. Stand. Technol.* 121, 238.
- Bell, I. H., Satyro, M., Lemmon, E. W., 2018. Consistent Twu Parameters for More than 2500 Pure Fluids from Critically Evaluated Experimental Data. *J. Chem. Eng. Data.*

- 58 Bell, I. H., Wronski, J., Quoilin, S., Lemort, V., 2014. Pure and
59 Pseudo-pure Fluid Thermophysical Property Evaluation and
60 the Open-Source Thermophysical Property Library Cool-
61 Prop. *Ind. Eng. Chem. Res.* 53 (6), 2498–2508. 44
- 62 Ben Adamson, B., Airah, M., 1998. Dimethyl ether as an R12
63 replacement. In: *Proceeding of IIF-IIR conference (Com-*
64 *missions B1, B2, E1 and E2)*, Osslø, Norway. pp. 610–17. 47
- 65 Benmansour, S., Richon, D., 1999. Vapor-Liquid Equilibria
66 and Densities of the Binary Refrigerant Mixture Composed
67 of Pentafluoroethane (R 125) and 1,1,1,2-Tetrafluoroethane
68 (R 134a) at Temperatures Between 253 K and 303 K and
1 Pressures up to 20 MPa (10402 data points). *Experimental*
2 *Data and Correlations*,. *ELDATA: The International Elec-*
3 *tronic Journal of Physico-Chemical Data* 5, 117–126. 54
- 4 Benoiel, R. W., 1941. Some Physical Constants of Seven Four-
5 Carbon-Atom Hydrocarbons and Neopentane. Ph.D. thesis,
6 Pennsylvania State University. 57
- 7 Bobbo, S., Stryjek, R., Elvassore, N., Bertucco, A., 1998. A re-
8 circulation apparatus for vapor-liquid equilibrium measure-
9 ments of refrigerants. Binary mixtures of R600a, R134a and
10 R236fa. *Fluid Phase Equilib.* 150-151, 343–352. 61
- 11 Bondi, A., 1968. *Physical Properties of Molecular Liquids,*
12 *Crystals, and Glasses.* Wiley, New York. 63
- 13 Buecker, D., Wagner, W., 2006. Reference Equations of State
14 for the Thermodynamic Properties of Fluid Phase n-Butane
15 and Isobutane. *J. Phys. Chem. Ref. Data* 35 (2), 929–1019. 66
- 16 Calado, J. C. G., McLure, I. A., Soares, V. A. M., 1978. Sur-
17 face Tension for Octafluorocyclobutane, n-Butane and their
18 Mixtures from 233 K to 254 K, and Vapor Pressure, Excess
19 Gibbs Function, and Excess Volume for the Mixtures at 233
20 K. *Fluid Phase Equilib.* 2, 199–213. 71
- 21 Carney, B. R., 1942a. Density of Liquified Petroleum Gas Hy-
22 drocarbons. *Hydrocarbon Process.* 21, 274. 73
- 23 Carney, B. R., 1942b. Density of Liquified Petroleum Gas Hy-
24 drocarbons, Their Mixtures and Three Natural Gasolines.
25 *Hydrocarbon Process.* 21, 84. 76
- 26 Chen, J., Fischer, K., Gmehling, J., 2002. Modification of
27 PSRK mixing rules and results for vapor-liquid equilibria,
28 enthalpy of mixing and activity coefficients at infinite dilu-
29 tion. *Fluid Phase Equilib.* 200 (2), 411–429. 80
- 30 Chen, J.-X., Chen, Z., Hu, P., Jiang, B., Li, Z.-H., 2007. Vapor-
31 Liquid Equilibria for the Binary System Pentafluoroethane
32 (HFC-125) + Isobutane (HC-600a) at Temperatures from
33 (243.15 to 333.15) K. *J. Chem. Eng. Data* 52, 2159–2162. 84
- 34 Coffin, C. C., Maass, O., 1928. The Preparation and Physical
35 Properties of .alpha.-, .beta.- and .gamma.-Butylene and Nor-
36 mal and Isobutane. *J. Am. Chem. Soc.* 50, 1427–1437. 87
- 37 Cragoe, C. S., 1943. Tech. Rep. LC-736, Natl. Bur. Stand. (U.
38 S.). 89
- 39 Dahlhoff, G., Pfennig, A., Hammer, H., Oorschot, M. v., 2000.
40 Vapor-Liquid Equilibria in Quaternary Mixtures of Dimethyl
Ether + n-Butane + Ethanol + Water. *J. Chem. Eng. Data* 45,
887–892.
- Dana, L. I., Jenkins, A. C., Burdick, H. E., Timm, R. C.,
1926. Thermodynamic Properties of Butane, Isobutane, and
Propane. *Refrig. Eng.* 12, 387.
- Fredenslund, A., Jones, R. L., Prausnitz, J. M., 1975. Group-
contribution estimation of activity coefficients in nonideal
liquid mixtures. *AIChE Journal* 21 (6), 1086–1099.
- Frey, K., Augustine, C., Ciccolini, R. P., Paap, S., Modell, M.,
Tester, J., 2007. Volume translation in equations of state as a
means of accurate property estimation. *Fluid Phase Equilib.*
260 (2), 316–325.
- Fujimine, T., Sato, H., Watanabe, K., 1999. Bubble-Point Pres-
sures and Saturated- and Compressed-Liquid Densities of
the Binary R-125 + R-143a System. *Int. J. Thermophys.* 20,
911–922.
- Glos, S., Kleinrahm, R., Wagner, W., 2004. Measurement of
the (p, rho, T) relation of propane, propylene, n-butane, and
isobutane in the temperature range from (95 to 340) K at
pressures up to 12 MPa using an accurate two-sinker den-
simeter. *J. Chem. Thermodyn.* 36, 1037–1059.
- Gmehling, J., 1985. Dortmund Data Bank-Basis for the devel-
opment of prediction methods. *CODATA Bulletin* (58), 56–
64.
- Haynes, W. M., Hiza, M. J., 1976. Orthobaric liquid densities
of normal butane from 135 to 300 K as determined with a
magnetic suspension densimeter. *Adv. Cryog. Eng.* 21, 516–
21.
- Haynes, W. M., Hiza, M. J., 1977. Measurements of the Ortho-
baric Liquid Densities of Methane, Ethane, Propane, Isobu-
tane, and Normal Butane. *J. Chem. Thermodyn.* 9, 179–187.
- Higashi, Y., 1999a. Vapor- Liquid Equilibrium, Coexistence
Curve, and Critical Locus for Pentafluoroethane + 1,1,1,2-
Tetrafluoroethane (R125/R134a). *J. Chem. Eng. Data* 44,
328–332.
- Higashi, Y., 1999b. Vapor-Liquid Equilibrium, Coexistence
Curve, and Critical Locus for Pentafluoroethane + 1,1,1-
Trifluoroethane (R125/R143a). *J. Chem. Eng. Data* 44, 333–
337.
- Higuchi, M., Higashi, Y., 1995. Measurements of the Vapor-
Liquid Equilibrium for Binary R-125/134a,. In: *Proc. 16th*
Japan Symp. Thermophys. Prop. pp. 5–8.
- Holcomb, C., Magee, J. W., Scott, J. L., Outcalt, S. L., Haynes,
W. M., 1998. Selected Thermodynamic Properties for Mix-
tures of R-32 R-125 R-134A R-143A R-41 R-290 and R-
744. Tech. Rep. Technical Note 1397, NIST.
- Holcomb, C. D., Magee, J. W., Haynes, W. M., 1995. Gas Pro-
cessors Association Project. Tech. Rep. 916, Research Re-
port RR-147.
- Hsu, J., Nagarajan, N., Robinson Jr., R. L., 1985. Equilibrium
Phase Compositions, Phase Densities and Interfacial Ten-

- sions for CO₂ + Hydrocarbon Systems. 1. CO₂ + n-Butane. *J. Chem. Eng. Data* 30, 485–491.
- Ikeda, T., Higashi, Y., 1995. Determination of the critical parameters for new refrigerant R-507 and R-407C. In: 16th Japan Symp. Thermophys. Prop. pp. 169–172.
- ISO 817:2014(en), 2000. Refrigerants – Designation and safety classification. Standard, International Organization for Standardization, Geneva, CH.
- Jaubert, J.-N., Mutelet, F., 2004. VLE predictions with the Peng-Robinson equation of state and temperature dependent kij calculated through a group contribution method. *Fluid Phase Equilibria* 224 (2), 285–304.
- Jaubert, J.-N., Privat, R., Guennec, Y. L., Coniglio, L., 2016. Note on the properties altered by application of a Pénélox-type volume translation to an equation of state. *Fluid Phase Equilib.* 419, 88–95.
- Ji, W.-R., Lempe, D., 1997. Density improvement of the SRK equation of state. *Fluid Phase Equilibria* 130 (1-2), 49–63.
- Kaminishi, G.-I., Yokoyama, C., Takahashi, S., 1988. Saturated liquid densities of n-butane-isobutane, n-butane-propane, isobutane-propane and n-butane-isobutane-propane mixtures. *Sekiyu Gakkaishi* 31, 433–8.
- Kato, R., Nishiumi, H., 2006. Vapor liquid equilibria and critical loci of binary and ternary systems composed of CH₂F₂, C₂H₂F₄ and C₂H₂F₆. *Fluid Phase Equilib.* 249, 140–146.
- Kay, W. B., 1940. Pressure-Volume-Temperature Relations for n-Butane. *Ind. Eng. Chem.* 32, 358–360.
- Kayukawa, Y., Hasumoto, M., Kano, Y., Watanabe, K., 2005. Liquid-Phase Thermodynamic Properties for Propane (1), n-Butane (2), and Isobutane (3). *J. Chem. Eng. Data* 50, 556–564.
- Kim, C. N., Park, Y. M., 1999. Vapor-liquid equilibrium of HFC-32/134 a and HFC-125/134a systems. *Int. J. Thermophys.* 20, 519–530.
- Kishizawa, G., Sato, H., Watanabe, K., 1999. Measurements of Saturation Densities in Critical Region and Critical Loci for Binary R-32/125 and R-125/143a Systems. *Int. J. Thermophys.* 20, 923–932.
- Kleemiss, M., 1997. Fortschrittsberichte VDI: Thermodynamic Properties of Two Ternary Refrigerant Mixtures: Measurements and Equations of State. Tech. Rep. Reihe 19 Nr. 98, VDI Verlag GmbH.
- Klosek, J., McKinley, C., 1968. Densities of LNG and of Low Molecular Weight Hydrocarbons. In: Proc. First Int. Conference on LNG.
- Kobayashi, M., Nishiumi, H., 1998. Vapor-liquid equilibria for the pure, binary and ternary systems containing HFC32, HFC125 and HFC134a. *Fluid Phase Equilib.* 144, 191–202.
- Kumagai, A., Takahashi, S., 1995. Viscosity and density of liquid mixtures of n-alkanes with squalane. *Int. J. Thermophys.* 16, 773–779.
- Kunz, O., Klimeck, R., Wagner, W., Jaeschke, M., 2007. The GERG-2004 Wide-Range Equation of State for Natural Gases and Other Mixtures. VDI Verlag GmbH.
- Le Guennec, Y., Lasala, S., Privat, R., Jaubert, J. N., 2016a. A consistency test for alpha-functions of cubic equations of state. *Fluid Phase Equilib.* 427, 513–538.
- Le Guennec, Y., Privat, R., Jaubert, J.-N., 2016b. Development of the translated-consistent tc-PR and tc-RK cubic equations of state for a safe and accurate prediction of Volumetric, energetic and saturation properties of pure compounds in the sub- and super-critical domains. *Fluid Phase Equilibria* 429, 301–312.
- Lee, B. G., Park, J. Y., Lim, J. S., Lee, Y. W., Lee, C. H., 2000. Vapor-liquid equilibria for isobutane + pentafluoroethane (HFC-125) at 293.15 to 313.15 K and + 1,1,1,2,3,3,3-heptafluoropropane (HFC-227ea) at 303.15 to 323.15 K. *J. Chem. Eng. Data* 45, 760–763.
- Legatski, T., Nelson, W., Dean, M., Fruit, L., 1942. Densities of Liquefied Petroleum Gases. *Ind. Eng. Chem.* 34, 1240–1243.
- Lemmon, E. W., Bell, I. H., Huber, M. L., McLinden, M. O., 2018. NIST Standard Reference Database 23: Reference Fluid Thermodynamic and Transport Properties-REFPROP, Version 10.0, National Institute of Standards and Technology. <http://www.nist.gov/srd/nist23.cfm>.
- Lim, J. S., Park, J. Y., Lee, B. G., Lee, Y. W., Kim, J. D., 2000. Reply to Comments by Stanislaw K. Malanowski and Roman Stryjek on *J. Chem. Eng. Data* 1999, 44, 1226-1230. *J. Chem. Eng. Data* 45, 1219–1221.
- Lopez-Echeverry, J. S., Reif-Acherman, S., Araujo-Lopez, E., 2017. Peng-Robinson equation of state: 40 years through cubics. *Fluid Phase Equilib.* 447, 39–71.
- Mathias, P. M., Copeman, T. W., 1983. Extension of the Peng-Robinson equation of state to complex mixtures: evaluation of the various forms of the local composition concept. *Fluid Phase Equilib.* 13, 91–108.
- McClune, C. R., 1976. Measurements of the Densities of Liquefied Hydrocarbons from 93 to 173 K. *Cryogenics* 16, 289–95.
- Miyamoto, H., Uematsu, M., 2007. Measurements of vapour pressures and saturated-liquid densities for n-butane at T = (280 to 424) K. *J. Chem. Thermodyn.* 39, 827–832.
- Mota-Babiloni, A., Navarro-Esbrí, J., Barragán-Cervera, Á., Molés, F., Peris, B., 2015. Analysis based on EU Regulation No 517/2014 of new HFC/HFO mixtures as alternatives of high GWP refrigerants in refrigeration and HVAC systems. *Int. J. Refrig* 52, 21–31.
- Nagel, M., Bier, K., 1995. Vapor-liquid equilibrium of ternary mixtures of the refrigerants R32, R125 and R134a. *Int. J. Refrig.* 18, 534–43.
- Niesen, V. G., 1989. (Vapor + liquid) equilibria and coexisting

- 92 densities of (carbon dioxide + n-butane) at 311 to 395 K. J. 41
93 Chem. Thermodyn. 21, 915–923. 42
- 94 Nishiumi, H., Ohno, T., 2000. High Pressure Vapor-liquid Equi- 43
95 libria and Critical Loci for the HFC125-HFC134a System. 44
96 Korean J. Chem. Eng. 17, 668–671. 45
- 97 Olds, R. H., Reamer, H. H., Sage, B. H., Lacey, W. N., 1944. 46
98 Phase Equilibria in Hydrocarbon Systems. Volumetric Be- 47
99 haviour of n-Butane. Ind. Eng. Chem. 36, 282. 48
- 100 Orrit, J. E., Laupretre, J. M., 1978. Density of liquefied natural 49
101 gas components. Adv. Cryog. Eng. 23, 573. 50
- 102 Outcalt, S., McLinden, M. O., 1995. Equations of State for the 51
1 Thermodynamic Properties of R32 (Difluoromethane) and 52
2 R 125 (Pentafluoroethane). Int. J. Thermophys. 32 (I). 53
- 3 Péneloux, A., Rauzy, E., Fréze, R., 1982. A consistent correc- 15
4 tion for Redlich-Kwong-Soave Volumes. Fluid Phase Equi- 16
5 lib. 8 (1), 7–23. 117
- 6 Peng, D.-Y., Robinson, D. B., 1976. A New Two-Constant 18
7 Equation of State. Ind. Eng. Chem. Fundam. 15 (1), 59–64. 119
- 8 Poling, B. E., Prausnitz, J. M., O'Connell, J. P., 2001. The Prop- 20
9 erties of Gases and Liquids, 5th edition. McGraw Hill. 1121
- 10 Prengle, H. W., Greenhaus, L. R., York, R., 1948. Thermody- 22
11 namic properties of n-Butane. Chem. Eng. Prog. 44, 863–81. 123
- 12 Privat, R., Jaubert, J.-N., Guennec, Y. L., 2016. Incorporation 24
13 of a volume translation in an equation of state for fluid mix- 25
14 tures: which combining rule? which effect on properties of 26
15 mixing? Fluid Phase Equilib. 427, 414–420. 1127
- 16 Qian, J.-W., Privat, R., Jaubert, J.-N., Coquelet, C., Ramjuge- 28
17 nath, D., 2017. Fluid-phase-equilibrium prediction of 29
18 fluorocompound-containing binary systems with the predic- 30
19 tive e-ppr78 model. International Journal of Refrigeration 31
20 73, 65 – 90. 1132
- 21 URL [http://www.sciencedirect.com/science/
22 article/pii/S0140700716302936](http://www.sciencedirect.com/science/article/pii/S0140700716302936)
- 23 Schmid, B., Gmehling, J., 2012. Revised parameters and typi-
24 cal results of the VTPR group contribution equation of state.
25 Fluid Phase Equilib. 317, 110–126.
- 26 Schmid, B., Gmehling, J., 2016. Present status of the group
27 contribution equation of state VTPR and typical applications
28 for process development. Fluid Phase Equilib. 425, 443–450.
- 29 Schmid, B., Schedemann, A., Gmehling, J., 2014. Extension of
30 the VTPR group contribution equation of state: Group in-
31 teraction parameters for additional 192 group combinations
32 and typical results. Ind. Eng. Chem. Res. 53 (8), 3393–3405.
- 33 Sliwinski, P., 1969. The lorentz-lorenz function of gaseous and
34 liquid ethane, propane and butane. Z. Phys. Chem. (Munich)
35 63, 263–79.
- 36 Soave, G., 1972. Equilibrium Constants from a Modified
37 Redlich-Kwong Equation of State. Chem. Eng. Sci. 27,
38 1197–1203.
- 39 Storn, R., Price, K., 1997. Differential Evolution – A Simple
40 and Efficient Heuristic for global Optimization over Contin-
uous Spaces. J. Global Opt. 11.
- Thompson, R. T., Miller, R. C., 1980. Densities and Dielectric
Constants of LPG Components and Mixtures at Cryogenic
Storage Conditions. Adv. Cryog. Eng. 26, 698.
- Twu, C. H., Bluck, D., Cunningham, J. R., Coon, J. E., 1991. A
cubic equation of state with a new alpha function and a new
mixing rule. Fluid Phase Equilib. 69, 33–50.
- Twu, C. H., Coon, J. E., Cunningham, J. R., 1995. A new gen-
eralized alpha function for a cubic equation of state Part 1.
Peng-Robinson equation. Fluid Phase Equilib. 105 (1), 49–
59.
- Uchida, H., Sato, H., Watanabe, K., 1999. Measurements of
Gaseous PVTx Properties and Saturated Vapor Densities of
Refrigerant Mixture R-125+R-143a. Int. J. Thermophys. 20,
97–106.
- Valderrama, J. O., 2003. The State of the Cubic Equations of
State. Ind. Eng. Chem. Res. 42 (8), 1603–1618.
- van der Waals, J. D., 1873. Over de Continuïteit van den Gas-
en Vloeïstoofstand. Ph.D. thesis, University of Leiden.
- Vasserman, A. A., Khasilev, I. P., Cymarnyi, V. A., 1989. Ta-
bles of recommended data. N-butane. Pressure and density
of liquid and gas at saturation. Tech. Rep. 604-kk, VNIKI.
- Wei, Y. S., Sadus, R. J., 2000. Equations of State for the Calcu-
lation of Fluid-Phase Equilibria. AIChE J. 46 (1), 169–196.
- Widiatmo, J. V., Fujimine, T., Sato, H., Watanabe, K.,
1997. Liquid Densities of Alternative Refrigerants Blended
with Difluoromethane, Pentafluoroethane, and 1,1,1,2-
Tetrafluoroethane. J. Chem. Eng. Data 42, 270–277.
- Widiatmo, J. V., Sato, H., Watanabe, K., 1995. Bubble-point
pressures and liquid densities of binary R-125 + R-143a sys-
tem. Int. J. Thermophys. 16, 801–810.